Imaging of Charged Micropatterned Monolayer Surfaces by Chemical Force Microscopy

Tomoyuki Koga, Hideyuki Otsuka, and Atsushi Takahara*

Institute for Materials Chemistry and Engineering, Kyushu University, 6-10-1 Hakozaki, Higashi-ku, Fukuoka 812-8581

Received March 10, 2005; E-mail: takahara@cstf.kyushu-u.ac.jp

Chemical force microscopy (CFM) was applied for the lateral force microscopic imaging of micropatterned organosilane monolayer surfaces with oppositely charged phases using chemically modified cantilever tips. Chemically modified cantilever tips with oxidized mercaptosilane, aminosilane, and unmodified cantilever tip were employed as a tip for CFM. Lateral force imaging of the micropatterned surface with opposite charge was successfully achieved by controlling the pH of the aqueous solution in consideration of the electrostatic condition of functional groups on the cantilever tip and substrate surface.

Over the past decade, a direct estimation technique of surface physicochemical properties has been expected to obtain useful information for various materials functionality, such as biocompatibility[1] and wettability.[2] It is well known that scanning force microscopy (SFM) has an advantage over optical and electron microscopy for investigating the physicochemical properties of materials surfaces by direct detection of the material surface information, such as frictional properties[3] and adhesive properties.[4]

Information about the surface functional groups is necessary in order to understand the relationship between the chemical composition of the material surface and those surface functional properties. Therefore, a chemical force microscope (CFM), which is one of the SFM family, has attracted much attention as an excellent technique for a direct determination of the specific chemical interaction between a cantilever tip surface modified with functional groups and a material surface as pull off force and lateral force.[5–19] In a CFM study, objective functional groups were identified by detecting any difference of the observed interactive force, such as a hydrophobic interaction and hydrogen bonds, in a region that is greater than that in the other regions. Lieber et al.[9–12] and Fujihira et al.[13–17] have reported that the two-dimensional distribution of different terminal functional groups of the monolayer surface can be imaged as a magnitude of lateral force or pull off force by using CFM through a hydrophobic interaction or a chemical interaction due to the hydrogen bonds.

In the case of ionized material surfaces, the intensity of the electrostatic interaction between the cantilever tip and the substrate surface strongly depends on the ionization state on both charged materials surfaces. Some studies have reported the sensing and imaging of an electrostatic interaction between the cantilever tip and the substrate surface. Hadziioannou et al.[20,21] have investigated the identification of the surface distribution of ionizable functional groups through an LFM observation. In this CFM study, the recognition of the relative difference of the electrostatic condition was a key to distinguish each micropatterned phase. Furthermore, Lieber et al.[11] have

also reported a pH dependence of the electrostatic condition of a substrate surface modified with ionizable functional groups based on the pull off force measurement. However, previous studies have not considered how to detect the electrostatic attractive force among the surface of the cantilever tip and an ionized surface because of the pH-dependent contribution of the tip functionality to the tip-substrate attractive force.

In the present paper, the authors report on the imaging of negatively and positively charged phases in a micropatterned surface by LFM to detect a specific electrostatic interaction using a cantilever tip with negatively and positively chargeable surface modifiers. The pH dependence of the sensitivity in LFM measurements is also discussed in acidic aqueous solution and pure water.

Experimental

Materials.   Organosilane compounds (butyltrimethoxysilane [$CH_3(CH_2)_3Si(OCH_3)_3$, BTMS], [3-(2-aminoethylamino)propyl]-(dimethoxy)methylsilane [$H_2N(CH_2)_2NH(CH_2)_3SiCH_3(OCH_3)_2$, AEAPDMS],   3-mercaptopropyltrimethoxysilane   [$HS(CH_2)_3Si(OCH_3)_3$, MTS], and octadecyltrichlorosilane [$CH_3(CH_2)_{17}SiCl_3$, OTS]) were used as surface modifiers. The OTS was purified by vacuum distillation. Toluene (Nacalai Tesque, Inc.) was refluxed with sodium for 6 h and distilled, and bicyclohexyl (Tokyo Kasei, Co., Ltd.) was dried with molecular sieves. The BTMS, AEAPDMS, MTS, and ethanol (Wako Pure Chemical Industries, Co., Ltd.), concentrated H_2SO_4 (Nacalai Tesque, Inc.), and 30% H_2O_2 (Santoku Chemical Industries, Co., Ltd.) were used as received without any further purification. Water for the CFM and contact angle measurements was purified with the NanoPure Water system (Millipore, Inc.). HCl aq was used to adjust the pH of an aqueous solution using CFM measurements. The substrates used in this study were Si-wafers from the Sumitomo Mitsubishi Silicon Corporation, Co., Ltd. (one side polished, thickness of 0.5 mm). Aluminum substrates were purchased from Nilaco Co., Ltd.

Sample Preparation.   The Si-wafers were soaked in a mixed solution of concentrated H_2SO_4 and 30% H_2O_2 (70/30, v/v) at 363 K for 1 h.[22] The treated Si-wafers were then rinsed with dis-

tilled water and ethanol. After they were dried in vacuo, the substrates were irradiated to clean by a vacuum ultraviolet ray (VUV, $\lambda = 172$ nm, a Xe excimer lamp, Ushio Electric, UER20-172) for 10 min at a pressure of 15 mmHg in order to remove any organic contamination.[23–31] The aluminum substrate was also cleaned by irradiation with a VUV-ray before surface modification.

The BTMS, AEAPDMS, and MTS monolayers were prepared by the chemical vapor adsorption (CVA) method.[23–31] The substrates were placed together with a 0.2 mL of BTMS or a 0.42 mL of 0.125 vol% AEAPDMS or MTS toluene solution into a 65 mL of Teflon™ container in a N_2 atmosphere. The container was then sealed with a cap and another stainless container. The stainless container was placed in an oven that was maintained at 373 K for 2 h. After a heating treatment, the substrates were taken from the container and immediately rinsed with ethanol (for BTMS) or toluene (for AEAPDMS and MTS). Finally, the substrates were dried in vacuo.

The MTS modified surface was irradiated by a UV-ray ($\lambda = 254$ nm, Spectronics Co., Ltd., ENF-240 C/J) for over 10 h in air in order to transform terminal mercapto groups on the MTS monolayer into sulfonic acid groups by photooxidation.[27,32]

The OTS monolayer was prepared onto the Si-wafer substrate from a 5 mM OTS bicyclohexyl solution using the chemisorption method in a N_2 atmosphere at room temperature for 1 h.[33,34] The Si-wafer substrate was rinsed with the bicyclohexyl, toluene, and ethanol. Finally, the samples were dried in vacuo.

Micropatterned samples were prepared using a combination of the photolithography method and the CVA method.[23–31] Figure 1 shows the fabrication process of a micropatterned organosilane monolayer. Table 1 gives the composition of the multicomponent organosilane monolayers used in this paper. Organosilane monolayers with lower reactive terminal groups were prepared early. First, an organosilane monolayer [BTMS, Oxidized MTS, or OTS] prepared on a Si-wafer surface was placed in an evacuated vacuum chamber. The sample was then covered with a photomask

(Toyo Precision Parts MFG. Co., Ltd., 20 mm × 20 mm square, 4 μm width Cr pattern, 2 μm width slit with a 20 mm line length) to prepare for irradiation by VUV-rays. A cylindrical stainless-steel weight was put on the photomask to achieve contact of the photomask to the sample surface. The samples were irradiated for 30 min with VUV-rays generated by a Xe excimer lamp in order to photodecompose the first organosilane monolayer. The patterned sample was sonicated for 5 min in ethanol and then dried in vacuo. A second organosilane monolayer [Oxidized MTS or AEAPDMS] was immobilized on the photodecomposed area, which was coated by silanol groups as a residue of a photodecomposed organosilane monolayer. Furthermore, a third organosilane monolayer [AEAPDMS] was prepared on the photodecomposed area by a photolithography method, resulting in crossline micropatterns on the substrate's surface. Finally, the obtained micropatterned organosilane monolayer with first and second organosilane monolayer phases were rinsed in toluene and ethanol, and then dried in vacuo.

X-ray Photoelectron Spectroscopy.   The formation of the sulfonic acid groups on the MTS monolayer after the irradiation of a UV-ray was identified by X-ray photoelectron spectroscopy (XPS) with the Phi ESCA 5800 system (Physical Electronics Inc.). The XPS measurement was performed with a monochromatized Al Kα X-ray source at 14 kV and 24 mA. The emission angle of photoelectrons was set to be 45 deg. The aluminum substrate irradiated with VUV-rays was used instead of a Si-wafer for the XPS measurement in order to remove the background derived from the Si_{2p} peak overlapped with the S_{2p} peak.

Contact Angle Measurement.   In order to identify the formation of sulfonic acid groups on the MTS monolayer, and to estimate the surface free energy of the organosilane monolayer, static contact angle measurements were carried out using water and diiodomethane as a probe liquid. Calculation of surface free energy was conducted based on Owens and Wendt's method.[35] The static contact angles of the monolayers against water and methyl-
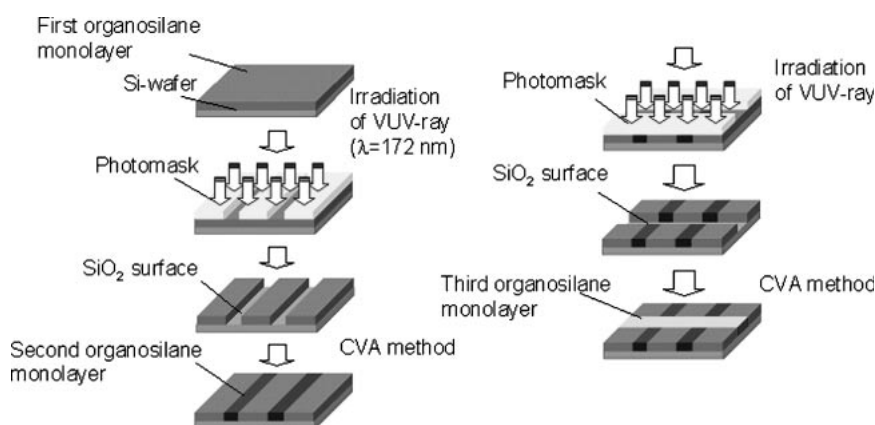

Fig. 1.   The fabrication process of a micropatterned organosilane monolayer.

Table 1.   The Composition of the Multicomponent Organosilane Monolayers

Sample	First organosilane monolayer	Second organosilane monolayer	Third organosilane monolayer
BTMS/Oxidized MTS	BTMS	Oxidized MTS	
BTMS/AEAPDMS	BTMS	AEAPDMS	
Oxidized MTS/AEAPDMS	Oxidized MTS	AEAPDMS	
OTS/Oxidized MTS/AEAPDMS	OTS	Oxidized MTS	AEAPDMS

T. Koga et al.

Bull. Chem. Soc. Jpn., **78**, No. 9 (2005)   1693

ene iodide were measured by a home-made system at room temperature.

Lateral Force Imaging with a Chemically Modified Cantilever Tip. Lateral force measurements for identifying of the micropatterned functional groups were conducted by atomic force microscopy (AFM, SPA-400, SII NanoTechnology Inc.). A 100 $\mu m \times 100 \mu m$ scanner and a Si_3N_4 tip on a cantilever with a spring constant of 0.09 $N\,m^{-1}$ were used. The Si_3N_4 cantilever tip with a radius R of curvature smaller than 20 nm was used in this study. The scan rate of the lateral force measurement was 10.0 $\mu m\,s^{-1}$, and the tip loads were 1.0 nN.

The SiO_2 layer of the cantilever's surface was chemically modified with either oxidized MTS or AEAPDMS by using the CVA method. Unmodified cantilever tips were also used in this study. The advantage of the CVA method is that it inflicts less damage on the cantilever tips due to the capillary force during handling compared with the chemisorption method in the solution phase. The cantilever surface can be uniformly modified with the organosilane monolayer, because the organosilane monolayer prepared by the CVA method has few aggregations and defects on their surface.[29] The cantilever tips were cleaned by irradiation with VUV-rays before modification. The CFM observation was carried out based on the electrostatic interaction between the monolayer surface and the cantilever tip surface. Figure 2 is a schematic drawing of the electrostatic interaction between a micropatterned surface with opposite charge and a chemically modified cantilever tip. All CFM measurements were carried out in the pH-controlled aqueous solutions (pH = 2.9 HCl aq and pH = 7.3 water). One hundred lateral force data were collected in order to calculate the lateral force value as a number average.

Results and Discussion

Identification of Oxidation of Terminal Mercapto Groups. The monolayers prepared from organosilane compounds are very stable against mechanical, thermal, and environmental change, and show no exchange reaction, unlike in the case of alkanethiol monolayer, because the organosilane compounds were immobilized onto the material surface with hydroxyl groups by a covalent bond and multiple hydrogen bonds.[36,37] Therefore, the organosilane compounds have attracted much attention as a surface modifier for a cantilever tip. The surface modification of a cantilever tip by an organosilane compound was carried out through the CVA method. The CVA method has been expected as surface modification
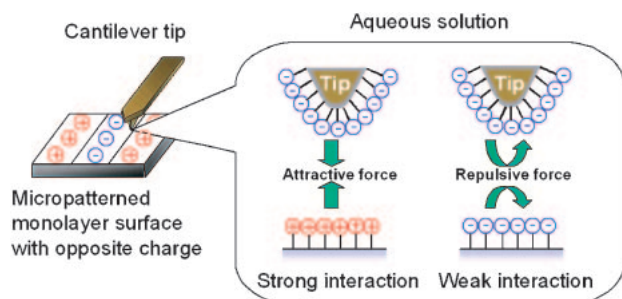
technique for the microscopic structure because the vapor is easy to penetrate into the nanoscale gap compared with a solution.[38] If we consider the interaction between monolayer surface and a liquid, a gold-coated layer influences the wetting behavior of the liquid because of the large Hamaker constant, A, of the gold-coated surface ($A_{\text{Au/alkanethiol monolayer-air}} = -1.1 \times 10^{-19}$ J) compared with that of a SiO_2 surface ($A_{\text{SiO}_2/\text{alkylsilane monolayer-air}} = -1.0 \times 10^{-20}$ J).[39] For example, Abbott et al. reported that the influence of the van der Waals force from a gold-coated surface is larger than that originating from a SiO_2 surface.[39] The large van der Waals force originated from gold might influence the tip-surface interaction. Thus, the direct coating of organosilane compounds on a Si_3N_4 cantilever tip can avoid this strong interaction compared with a gold-coated cantilever tip modified with alkanethiol compounds.

The formation of a sulfonic acid group on a MTS monolayer surface was also identified by XPS and contact angle measurements. The transformation of terminal mercapto groups into sulfonic acid groups was estimated by XPS measurements. Figure 3 shows the XPS S_{2p} spectra of a MTS monolayer prepared on an aluminum substrate surface before and after the irradiation of UV-rays. In Fig. 3, the S_{2p} peaks originating from mercapto groups and sulfonic acid groups were observed at 163.3 and 169.0 eV, respectively.[27,32] The oxidation of mercapto groups before the irradiation of UV-rays can be attributed to natural oxidation by oxygen in air and light. On the other hand, the S_{2p} peak derived from mercapto groups completely disappeared after the irradiation of UV-rays. In other words, almost all mercapto groups were converted into sulfonic acid groups. In the XPS measurement, the C_{1s} peak of the functional groups derived from the oxidation of CH_2 groups could not be observed in the MTS monolayer after the irradiation of UV-ray. Therefore, it is expected that the MTS monolayer did not suffer any serious damage by the irradiation of UV-rays.

The formation of sulfonic acid groups was also evaluated by contact angle measurements. The contact angle of water droplets on a MTS monolayer surface prepared on a Si-wafer substrate decreased after the irradiation of UV-rays ($\lambda = 254$ nm)
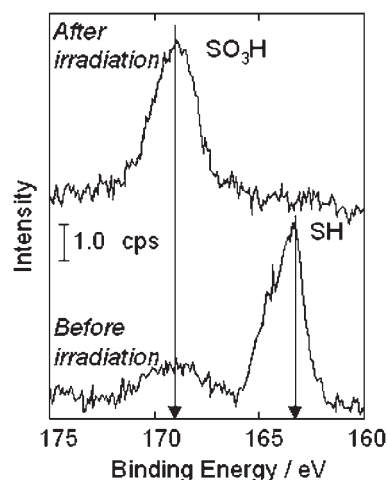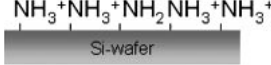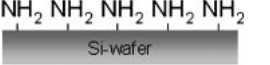

Fig. 2. Schematic drawing of the electrostatic interaction between a micropatterned surface with opposite charge and a chemically modified cantilever tip. This is a case in which the cantilever tip surface is covered with negatively charged functional groups.
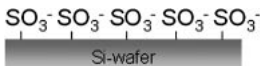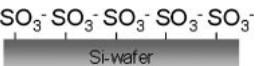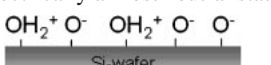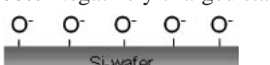

Fig. 3. The XPS S_{2p} spectra of a MTS monolayer prepared on an aluminum substrate surface before and after the irradiation of a UV-rays ($\lambda = 254$ nm).

Table 2. Schematic Representation of the Ionization State of Surface Amino, Sulfonic Acid, and Silanol Groups on the AEAPDMS, oxidized MTS, and an Unmodified Cantilever Tip Surface

	pH = 2.9 HCl aq	pH = 7.3 Water
Amino groups on AEAPDMS monolayer surface	80% Positively charged state $NH_3^+ NH_3^+ NH_2 NH_3^+ NH_3^+$ Si-wafer	Uncharged state $NH_2\ NH_2\ NH_2\ NH_2\ NH_2$ Si-wafer
Sulfonic acid groups on oxidized MTS monolayer surface	ca. 100% Negatively charged state $SO_3^-\ SO_3^-\ SO_3^-\ SO_3^-\ SO_3^-$ Si-wafer	ca. 100% Negatively charged state $SO_3^-\ SO_3^-\ SO_3^-\ SO_3^-\ SO_3^-$ Si-wafer
Silanol groups on unmodified cantilever tip surface	Electrically almost neutral state $OH_2^+\ O^-\ \ OH_2^+\ O^-\ \ O^-$ Si-wafer	ca. 100% Negatively charged state $O^-\ \ O^-\ \ O^-\ \ O^-\ \ O^-$ Si-wafer

due to the formation of sulfonic acid groups. The water contact angle became constant after the irradiation of UV-rays for over 9.5 h (before irradiation) 71.8 deg; after irradiation for over 9.5 h (31.7 deg).

Electrostatic Condition of Surface Functional Groups. Lieber et al.,[11] Hadziioannou et al.,[20,21] and the authors[27] have reported that pK_a of surface functional groups in an organic ultrathin film shifts compared with free functional groups. This is due to stabilization by hydrogen bonds among the neighboring condensed functional groups,[11,20,21,28,40] and the shielding of functional groups by hydrophobic methylene groups from protons in aqueous media.[27] The pK_a of surface functional groups was estimated by evaluating the pH dependence of the pull off force between the cantilever tip surface and the substrate surface modified with the same functional groups in a pH-controlled aqueous solution.[11,20,21,27] We have previously reported that the pK_a of amino groups on the AEAPDMS surface is ca. 4.0.[27] In the case of amino groups in an AEAPDMS monolayer, we could estimate the degrees of the ionization state, f, by using

$$pH = pK_a + \log[(1 - f)/f]. \tag{1}$$

In the case of $f \approx 0$, it is assumed that the surface amino groups are not protonated at all. In the case of $f \approx 1$, it is presumed that almost all of the surface amino groups are protonated. When pK_a is ca. 4.0, the degree of the ionization state of the amino groups in the AEAPDMS monolayer is approximately 80% at pH = 2.9, and almost 0% at pH = 7.3.

The authors also estimated the pK_a value of sulfonic acid groups on an oxidized MTS monolayer by a similar method; however, a large variation of the pull off force could not be detected at pH = 1.5–8.0. This is probably due to an electrostatic repulsive force among highly ionized sulfonic acid groups in aqueous solutions. Therefore, it is expected that the surface sulfonic acid groups on the oxidized MTS monolayer are almost 100% ionized at pH = 2.9 and pH = 7.3.

The ionization state of an unmodified cantilever tip surface with silanol groups was estimated based on a reported value. The electrostatic condition of silanol groups depends on their zero-point of charge (ZPC). Parks[41] has reported that the ZPC of silanol groups on a quartz surface is below 2.4 at 298 K under atmospheric pressure. Therefore, it is considered

that the silanol groups on an unmodified cantilever tip surface were electrically almost neutral at pH = 2.9 and ca. 100% negatively charged at pH = 7.3. Table 2 summarizes the schematic representation of the ionization state of surface amino, sulfonic acid, and silanol groups on the AEAPDMS, oxidized MTS monolayer, and an unmodified cantilever tip surface, respectively.

Number of Interacting Molecules between the Tip and the Sample Surface. In order to discuss the influence of the terminal functional groups on the observed lateral force, it is important to clarify the number of interacted functional groups between the cantilever tip and the substrate surface. Therefore, we estimated the number of interacted organosilane molecules from the area of contact A. The area of contact A between the tip and sample surface was estimated by the Johnson–Kendall–Roberts (JKR) model.[13,42,43] According to the JKR model, the contact area between the tip and the sample, A, is given by

$$A = (R/K)^{2/3}(F_N + 3\pi R W_{12} + [6\pi W_{12} R F_N + (3\pi R W_{12})^2]^{1/2}), \tag{2}$$

where R is the radius of the cantilever tip (20 nm), F_N is the normal load force, which is the same as the tip loads in this paper, K is the elastic modulus of the contacting materials [$K = 4/\{3\pi(k_1 + k_2)\}$]. k_1 and k_2 are the elastic constants of the tip and the sample surfaces, that is

$$k_i = (1 - \nu_i^2)/\pi E_i \quad i = 1, 2, \tag{3}$$

where ν_i is the Poisson ratio and E_i is Young's modulus of the tip and the sample material. W_{12} is the work of pull off for separating the sample and tip. The work of pull off can be estimated by

$$W_{12} = \gamma_s + \gamma_t - \gamma_{st}, \tag{4}$$

where γ_s and γ_t are the surface free energies of the sample and tip, respectively, and γ_{st} is the interfacial free energy of the two contacting surfaces. If we consider the sample and tip combinations that have the same surface functional groups (for example, SO_3H/SO_3H and NH_2/NH_2 pairs), then $\gamma_{st} = 0$ and $\gamma_s = \gamma_t$, and it is possible to simplify Eq. 4 to $W_{st} = 2\gamma$, where γ in our case corresponds to the free energy of the surface in equilibrium with the solvent. For example, the
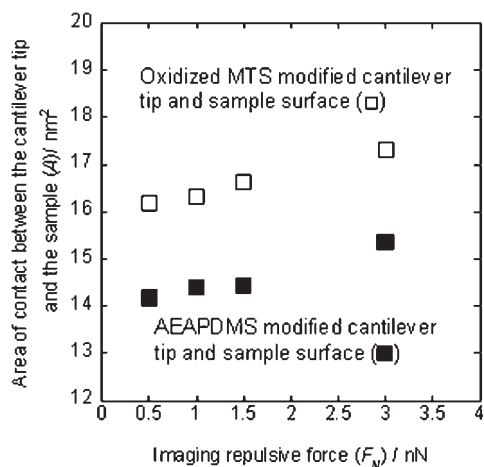
Fig. 4.   The imaging repulsive force, which corresponds to the contact load, (F_N) dependent calculated contact area *A* of oxidized MTS cantilever tip/oxidized MTS phase pair (open square) and AEAPDMS modified cantilever tip/AEAPDMS phase pair (filled square) based on JKR model.

γ values of the oxidized MTS monolayer and AEAPDMS monolayer surface, estimated by a static contact angle measurement, were 59.4 and 48.5 mJ m^{-2}, respectively. The reported Poisson ratio, ν and Young's modulus, E, of the Si$_3$N$_4$ cantilever tip, and the Si-wafer substrate surface (SiO$_2$) were 0.27, 0.17 and 294, and 70 GPa, respectively.[44,45] Thus, the area, *A*, of contact between the tip and the sample modified with same functional groups could be calculated as shown in Fig. 4. The F_N value was 1.0 nN in this study; thus, the areas of contact between the tip and the sample surface were 16.33 nm^2 (SO$_3$H/SO$_3$H) and 14.39 nm^2 (NH$_2$/NH$_2$), respectively. The number of interacting molecules between the tip and the sample surface was estimated from area occupied by each organosilane molecules on the material surface. Kojio et al. reported that the area occupied by organosilane molecules in the OTS monolayer with a hexagonal crystalline phase prepared by the Langmuir–Blodgett method was ca. 0.20 nm^2 molecules^{-1}.[46] Therefore, the estimated numbers of interacting molecules between the tip and the Si-wafer surface were ca. 82 (SO$_3$H/SO$_3$H) and ca. 72 (NH$_2$/NH$_2$), respectively, by assuming that the area occupied by oxidized MTS and AEAPDMS molecules in the monolayer was the almost same value estimated by Kojio et al. The number of interacting MTS molecules was almost equal to that of interacted AEAPDMS molecules. Thus, it is considered that the difference of CFM measurement in this study was mainly due to the difference of the terminal functional groups. However, we have reported that the organosilane monolayer prepared by the CVA method has a low molecular density compared with the crystalline OTS monolayer.[29] Thus, the actual number of interacting molecules between the tip and the Si-wafer surface was smaller than that estimated based on the area occupied by the organosilane molecules in the crystalline OTS monolayer.

CFM Imaging of a (Alkyl Groups/Sulfonic Acid Groups) Micropatterned Surface.   In order to investigate the recognition of the attractive and repulsive forces, the lateral force be-

tween the cantilevers modified with AEAPDMS or oxidized MTS and (BTMS/oxidized MTS) micropatterned surface was estimated. There is no difference between the BTMS monolayer and the oxidized MTS monolayer from the view point of the chemical structure, except for the terminal functional groups. Therefore, it is considered that the influence of the difference in the terminal functional groups can be investigated. Figure 5 shows (a), (c) LFM images and (b), (d) histograms of lateral force observed on the (BTMS/oxidized MTS) micropatterned surface in pH = 7.3 water [(a) and (b); with oxidized MTS modified cantilever tip, (c) and (d); with AEAPDMS modified cantilever tip]. In Figs. 5(a) and (b), a clear difference of magnitude of the lateral force was observed. The bright and dark areas in Fig. 5(a) correspond to the BTMS and the oxidized MTS monolayer phases, respectively. The authors reported that the sulfonic acid groups on oxidized MTS monolayer surface are negatively charged above pH = 1.5.[27] Conversely, the sulfonic acid groups on the substrate and the cantilever tip surface were negatively charged at pH = 7.3. Therefore, it is considered that the observed difference of the lateral force on the (BTMS/oxidized MTS) patterned surface is derived from the repulsive force between the cantilever tip and the micropatterned phases modified with sulfonic acid groups. On the other hand, in Figs. 5(c) and (d), the contrast in the LFM image was reversed by using the cantilever tip modified with AEAPDMS. The pK_a of amino groups on the AEAPDMS monolayer surface has been reported to be approximately ca. 4.0.[20] Thus, amino groups of AEAPDMS monolayer are not protonated at pH = 7.3. The observed difference of the lateral force on the (BTMS/oxidized MTS) surface is derived from the attractive force originating from the weak electrostatic attractive force between the unprotonated amino groups on the cantilever tip and the negatively charged sulfonic acid groups on the Si-wafer surface.

pH Dependent LFM Imaging of an Oppositely Charged Surface.   Figure 6 shows LFM images of an (oxidized MTS/AEAPDMS) micropatterned monolayer surface in pH = 2.9 HCl aq [(a); with the cantilever tip modified with oxidized MTS, (b); with the cantilever tip modified with AEAPDMS, (c); unmodified cantilever tip]. In Figs. 6(a) and (b), a clear difference of the lateral force between the oxidized MTS phase and the AEAPDMS one can be observed on the (oxidized MTS/AEAPDMS) micropatterned surface. In pH = 2.9 HCl aq, the sulfonic acid groups of oxidized MTS and the amino groups of AEAPDMS were negatively and positively charged, respectively. Therefore, this result apparently indicated that a clear contrast in the LFM image of the (oxidized MTS/AEAPDMS) micropatterned surface is due to the contribution of (1) the electrostatic attractive force among oppositely charged functional groups on the Si-wafer substrate and the cantilever tip surface; and (2) the electrostatic repulsive force among the ionized functional groups with the same charge on the Si-wafer substrate and the cantilever tip surface. On the other hand, a clear LFM image was not be obtained by an unmodified cantilever tip [Fig. 6(c)]. In consideration of Table 2, the silanol groups on the unmodified cantilever tip surface were electrically almost neutral at pH = 2.9. Therefore, the difference in the observed lateral force was not large with the unmodified cantilever tip due to the lack of an electro-
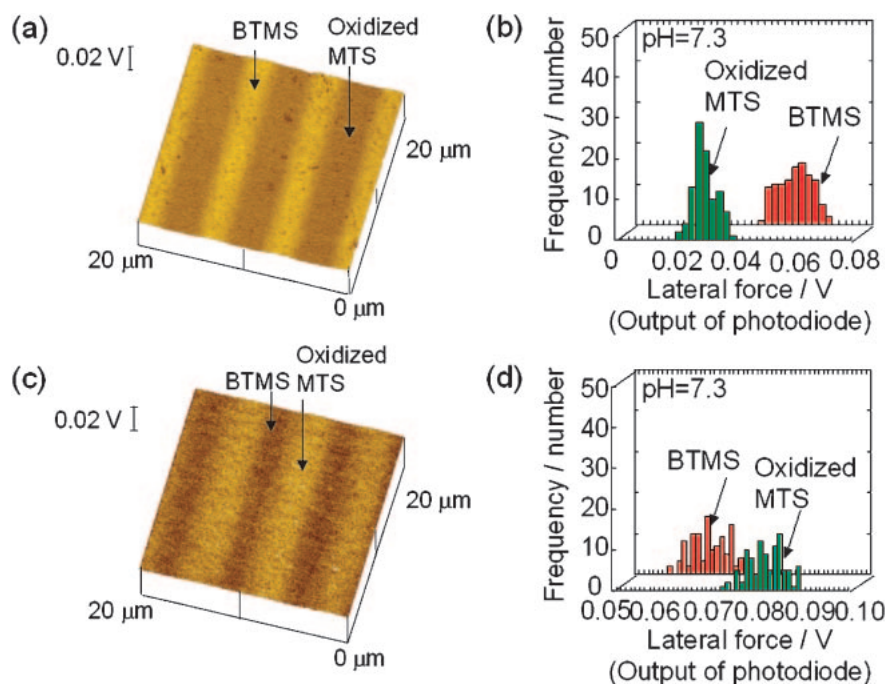
Fig. 5.   (a), (c) LFM images and (b), (d) histograms of the lateral force observed on the (BTMS/oxidized MTS) micropatterned surface in pH = 7.3 water. [(a) and (b); with the cantilever tip modified with oxidized MTS, (c) and (d); with the cantilever tip modified with AEAPDMS.]
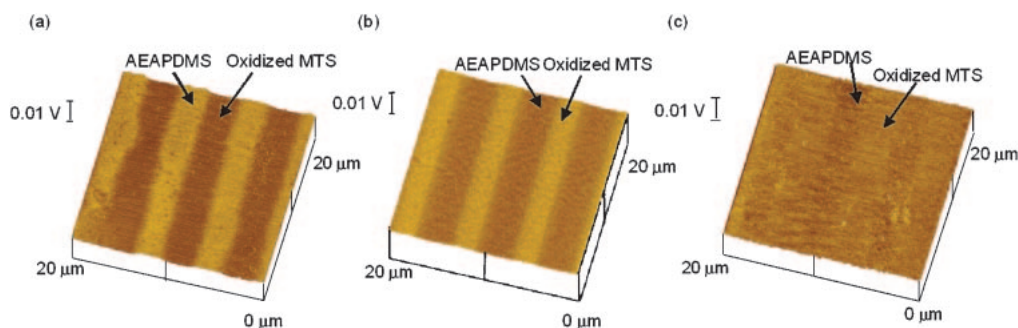

Fig. 6.   LFM images of an (oxidized MTS/AEAPDMS) micropatterned surface in pH = 2.9 HCl solution. [(a) by cantilever tip modified with oxidized MTS, (b) by cantilever tip modified with AEAPDMS, (c) by unmodified cantilever tip.]

static interaction between the unmodified cantilever tip and the ionized (oxidized MTS/AEAPDMS) micropatterned surface.

By using the cantilever tip modified with ionizable functional groups, relative differences in the lateral force could be changed by controlling the pH of the aqueous media. Figure 7 shows histograms of the lateral force observed on the (oxidized MTS/AEAPDMS) monolayer surface by using the cantilever tip modified with AEAPDMS in (a) pH = 2.9 HCl aq and (b) pH = 7.3 water. The data in Fig. 7(a) correspond to the LFM image of Fig. 6b. In the case of the cantilever tip modified with AEAPDMS, there was no large difference in the histograms of the lateral force at pH = 7.3 [Fig. 7(b)]. In pH = 7.3 water, almost all amino groups of the AEAPDMS monolayer were not protonated. Thus, the repulsive force due to the positive charge of amino groups was not observed between the cantilever tip and the micropatterned phase modified with AEAPDMS at pH = 7.3. Therefore, the difference of the lateral force between the oxidized MTS phase

and the AEAPDMS one was too small to be observed.

A Multi-Component Micropatterned Surface with Oppositely Charges and Hydrophobic Phase.   A multi-component micropatterned surface with charge could also be imaged using CFM. Figure 8 shows (a) an LFM image and (b) the histograms of the observed lateral force on the (OTS/oxidized MTS/AEAPDMS) monolayer surface, which has three phases with different surface chemistry, in pH = 7.3 water by the cantilever tip modified with oxidized MTS. As shown in Fig. 8, three different monolayer phases were clearly identified. The AEAPDMS phases are the brightest among three monolayer phases due to the weak electrostatic attractive force between the AEAPDMS monolayer and the cantilever surface modified with oxidized MTS. The origin of the difference of the lateral force value among the OTS phase and the oxidized MTS phase was explainable by the following two reasons. The first reason is the electrostatic repulsive force among a negatively charged cantilever tip modified with oxidized MTS and the negatively
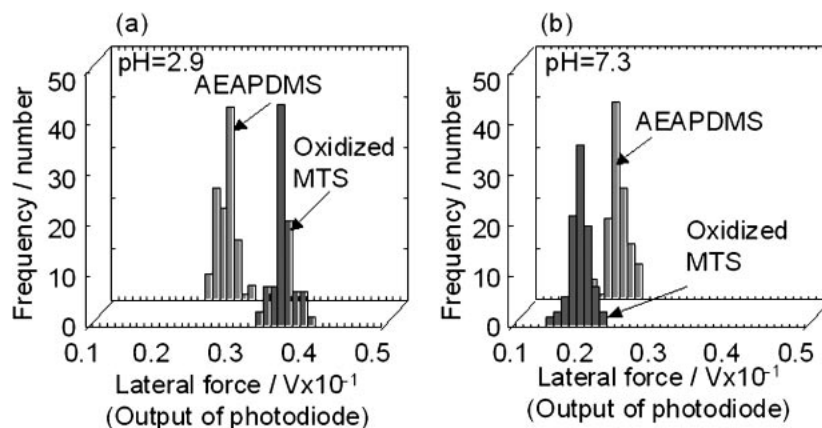
Fig. 7. Histograms of observed lateral force on the (oxidized MTS/AEAPDMS) micropatterned surface with cantilever tip modified with AEAPDMS in (a) pH = 2.9 HCl aq, (b) pH = 7.3 water.
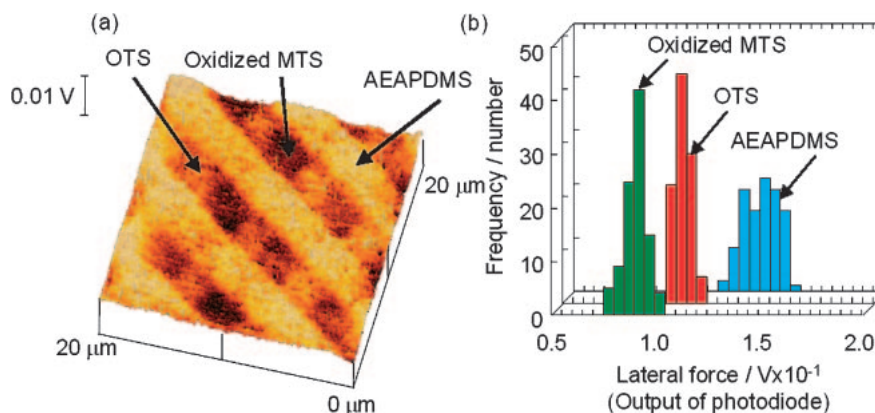

Fig. 8. (a) an LFM image and (b) histograms of the observed lateral force on the (OTS/oxidized MTS/AEAPDMS) monolayer surface by the cantilever tip modified with oxidized MTS in pH = 7.3 water.

charged sulfonic acid groups on the oxidized MTS phase. The second reason is the difference in the aggregation state of organosilane monolayers. Kojio et al. has reported that the observed lateral force on the organosilane monolayers with long alkyl chains depends on their molecular packing density and thermal molecular motion.[47,48] Thus, a large lateral force was observed on the crystalline organosilane monolayer with long alkyl chains, such as an OTS monolayer prepared by the chemisorption method from solution phase, because of the large shear strength due to their tightly packed alkyl chains and a decrease of the thermal molecular motion.[48] Taking into account the high molecular packing density and less-active thermal molecular motion of the alkyl chains of the OTS phase, the difference in the lateral force between the OTS phases and the oxidized MTS phases originated from the electrostatic repulsive force between the oxidized MTS phases and the cantilever tip surface modified with oxidized MTS, and the difference in the shear strength of long alkyl chains in the OTS phase due to the tightly packed molecular density and the small thermal molecular motion of the octadecyl groups.

Conclusion

The imaging of micropatterned charged monolayer surfaces was successfully achieved by using a lateral force measurement with a cantilever tip modified with oxidized MTS or AEAPDMS. This technique is based on the detection of an electrostatic attractive or repulsive force between the terminal functional groups of the monolayer surface and the cantilever surface. The magnitude of the lateral force could be controlled by optimizing the electrostatic condition of the terminal functional groups. It is expected that the CFM imaging technique based on the electrostatic interaction will become a powerful tool to understand the surface behavior of various charged material surfaces, such as biocompatible materials and template materials to area-selectively assemble and align the protein, microparticle, and polymer ultrathin films. Also, the CFM technique using an electrostatic interaction conducted in aqueous media is expected to make it possible to investigate the surface of biologically active materials, such as proteins and cells, because one can directly investigate the surface behavior of biomaterials alive under mild aqueous conditions.

References

1 a) "Biomaterials Science. An Introduction to Materials in Medicine," ed by B. D. Ratner, A. L. Hoffman, F. J. Schone, and J. E. Lemons, Academic Press (1996). b) "Biomedical Applications of Polymeric Materials," ed by T. Tsuruta, T. Hayashi, K. Kataoka, K. Ishihara, and Y. Kimura, CRC Press (1993).

2 a) J. Sagiv, *J. Am. Chem. Soc.*, **102**, 92 (1980). b) R. Maoz and J. Sagiv, *Thin Solid Films*, **132**, 135 (1985). c) S.-R. Ge, A. Takahara, and T. Kajiyama, *J. Vac. Sci. Technol., A*, **12**, 2530 (1994).

3 a) R. W. Carpick and M. Salmeron, *Chem. Rev.*, **97**, 1163 (1997). b) T. Kajiyama, I. Ohki, and A. Takahara, *Macromolecules*, **28**, 4768 (1995). c) A. Akabori, K. Tanaka, T. Kajiyama, and A. Takahara, *Macromolecules*, **36**, 4937 (2003).

4 a) K. Feldman, T. Tervoort, P. Smith, and D. Spencer, *Langmuir*, **14**, 372 (1998). b) W. A. Ducker, T. J. Senden, and R. M. Pashley, *Langmuir*, **8**, 1831 (1992). c) R. Ishiguro, D. Y. Sasaki, C. Pacheco, and K. Kurihara, *Colloids Surf., A*, **146**, 329 (1999).

5 A. Takahara, Y. Hara, K. Kojio, and T. Kajiyama, *Macromol. Symp.*, **166**, 271 (2001).

6 A. Takahara, Y. Hara, K. Kojio, and T. Kajiyama, *Colloids Surf., B*, **23**, 141 (2002).

7 T. Nakagawa, K. Ogawa, T. Kurumizawa, and S. Osaki, *Jpn. J. Appl. Phys.*, **32**, L294 (1993).

8 H. Takano, J. R. Kenseth, J. S.-S. Wong, J. C. O'Brien, and M. D. Porter, *Chem. Rev.*, **99**, 2845 (1999).

9 C. D. Frisbie, L. F. Rozsnyai, A. Noy, M. S. Wrighton, and C. M. Lieber, *Science*, **265**, 2071 (1994).

10 A. Noy, C. D. Frisble, L. F. Rozsnyai, M. S. Wrighton, and C. M. Lieber, *J. Am. Chem. Soc.*, **117**, 7943 (1995).

11 D. V. Vesenov, A. Noy, L. F. Rozsnyai, and C. M. Lieber, *J. Am. Chem. Soc.*, **119**, 2006 (1997).

12 A. Noy, C. H. Sanders, D. V. Vezenov, S.-S. Wong, and C. M. Lieber, *Langmuir*, **14**, 1508 (1998).

13 T. Miyatani, M. Horii, A. Rosa, M. Fujihira, and O. Marti, *Appl. Phys. Lett.*, **71**, 2632 (1997).

14 Y. Okabe, U. Akiba, and M. Fujihira, *Appl. Surf. Sci.*, **157**, 398 (2000).

15 Y. Okabe, Y. Furugori, M. Tani, U. Akiba, and M. Fujihira, *Ultramicroscopy*, **82**, 203 (2000).

16 M. Fujihira, Y. Tani, M. Furugori, U. Akiba, and Y. Okabe, *Ultramicroscopy*, **86**, 263 (2001).

17 M. Fujihira, M. Furugori, U. Akiba, and Y. Tani, *Ultramicroscopy*, **86**, 75 (2001).

18 R. C. Thomas, J. E. Houston, R. M. Crooks, T. Kim, and T. A. Michalske, *J. Am. Chem. Soc.*, **117**, 3830 (1995).

19 S. Kidoaki, Y. Nakayama, and T. Matsuda, *Langmuir*, **17**, 1080 (2001).

20 E. W. van der Vegte and G. Hadziioannou, *J. Phys. Chem. B*, **101**, 9563 (1997).

21 E. W. van der Vegte and G. Hadziioannou, *Langmuir*, **13**, 4357 (1997).

22 S.-R. Ge, A. Takahara, and T. Kajiyama, *J. Vac. Sci. Technol., A*, **12**, 2530 (1994).

23 T. Koga, H. Otsuka, and A. Takahara, *Chem. Lett.*, **2002**, 1196.

24 T. Koga, M. Morita, H. Sakata, H. Otsuka, and A. Takahara, *Int. J. Nanosci.*, **1**, 419 (2002).

25 A. Takahara, H. Sakata, M. Morita, T. Koga, and H. Otsuka, *Compos. Interfaces*, **10**, 489 (2003).

26 H. Sugimura, K. Ushiyama, A. Hozumi, and O. Takai, *Langmuir*, **16**, 885 (2000).

27 T. Koga, M. Morita, H. Otsuka, and A. Takahara, *Trans. Mater. Res. Soc. Jpn.*, **29**, 153 (2004).

28 A. Takahara, "Molecular Assembly Organosilanes, Encyclopedia of Nanoscience and Nanotechnology," ed by J. A. Schwarz, Dekker (2004), Vol. 3, p. 2031.

29 T. Koga, M. Morita, H. Ishida, H. Yakabe, S. Sasaki, O. Sakata, H. Otsuka, and A. Takahara, *Langmuir*, **21**, 905 (2005).

30 M. Morita, T. Koga, H. Otsuka, and A. Takahara, *Langmuir*, **21**, 911 (2005).

31 N. Saito, Y. Wu, K. Hayashi, H. Sugimura, and O. Takai, *J. Phys. Chem. B*, **107**, 664 (2003).

32 S. K. Bhatia, J. L. Texeria, M. Anderson, L. C. S. Lake, J. F. Calvert, J. H. Georger, J. J. Hickman, C. S. Dulcey, P. E. Schone, and F. S. Ligler, *Anal. Biochem.*, **208**, 197 (1993).

33 A. Takahara, K. Kojio, and T. Kajiyama, *Ultramicroscopy*, **91**, 203 (2002).

34 K. Kojio, A. Takahara, K. Omote, and T. Kajiyama, *Langmuir*, **16**, 3932 (2000).

35 D. K. Owens and R. C. Wendt, *J. Appl. Polym. Sci.*, **13**, 1741 (1969).

36 M. J. Hosteler, S. J. Green, J. J. Stokes, and R. W. Murray, *J. Am. Chem. Soc.*, **118**, 4212 (1996).

37 T. Gu, J. K. Whitesell, and M. A. Fox, *Chem. Mater.*, **15**, 1358 (2003).

38 G.-Y. Jung, Z. Li, W. Wu, Y. Chen, D. L. Olynick, S.-Y. Wang, W. M. Tong, and R. S. Williams, *Langmuir*, **21**, 1158 (2005).

39 W. J. Miller and N. L. Abbott, *Langmuir*, **13**, 7106 (1997).

40 Q. R. Huang, P. L. Dubin, C. N. Moorefield, and G. R. Newkome, *J. Phys. Chem. B*, **104**, 898 (2000).

41 G. A. Parks, "Equilibrium Concepts in Natural Water Systems," ed by W. E. Stumm, Advances in Chemistry Series–American Chemical Society, Washington D. C. (1967), Vol. 67, pp. 121–158.

42 K. L. Johnson, K. Kendall, and A. D. Roberts, *Proc. R. Soc. London, Ser. A*, **342**, 301 (1971).

43 Y. Sun, B. Akhremitchev, and G. C. Walker, *Langmuir*, **20**, 5837 (2004).

44 K. Kida, K. Kitamura, H. Chiba, and K. Yamakawa, *Int. J. Fatigue*, **27**, 165 (2005).

45 M. T. Kim, *Thin Solid Films*, **283**, 12 (1996).

46 K. Kojio, S.-R. Ge, A. Takahara, and T. Kajiyama, *Langmuir*, **14**, 971 (1998).

47 B. J. Briscoe and D. C. B. Evans, *Proc. R. Soc. London, Ser. A*, **380**, 389 (1982).

48 K. Kojio, A. Takahara, and T. Kajiyama, *Langmuir*, **16**, 9314 (2000).